JOURNAL OF MATERIALS SCIENCE 27 (1992) 4477–4482

Sintering and microstructure of silicon nitride prepared by plasma CVD

Y. MORIYOSHI, M. FUTAKI
National Institute for Research in Inorganic Materials, Namiki 1-1, Tsukuba, 305 Japan
N. EKINAGA, T. NAKATA
Tokai Carbon Co. Ltd, Fuji Laboratory, 410-14 Japan

Ultrafine Si_3N_4 powder with average particle size of 30 nm prepared by a thermal plasma CVD was sintered at 1750 °C in nitrogen for 1 h. The sintering behaviour of the powder was characterized by the crystallization of the powder and the resultant sintered bodies were observed with microscopes. It was found that the sinterability depended strongly on the green density and the degree of crystallization. If the powder was homogeneously mixed with sintering additives, it sintered to 98% density at 1750 °C in a nitrogen atmosphere. The microstructure of the sintered bodies observed by SEM indicated that they consist of needle-like grains with an aspect ratio of about 4. The microstructure of a thin film of the sintered body observed by TEM indicated that the grains with crystal habits were wet with liquid phase. TEM also clarified that two kinds of grain boundaries were present; one was wet with liquid phase along a grain boundary and the other was a coincident one without liquid phase. The lattice fringes of liquid phase suggested the presence of Y-apatite which would be generated during cooling.

1. Introduction

A previous review has shown that the sintering of Si_3N_4 has been studied by many workers [1–10]. We have, also previously reported the preparation of ultrafine Si_3N_4 powder by thermal plasma chemical vapour deposition (CVD) and its sintering behaviour [11]. As a result, the sinterability of the powder described as a function of temperature indicated the importance of green density, particle size, particle shape, and sintering additives. The obtained sinterability compared with commercially available Si_3N_4 powder was discussed. In this work, sintering and characterization of Si_3N_4 powder were carried out. The resultant sintered bodies were then observed with a transmission electron microscope (TEM).

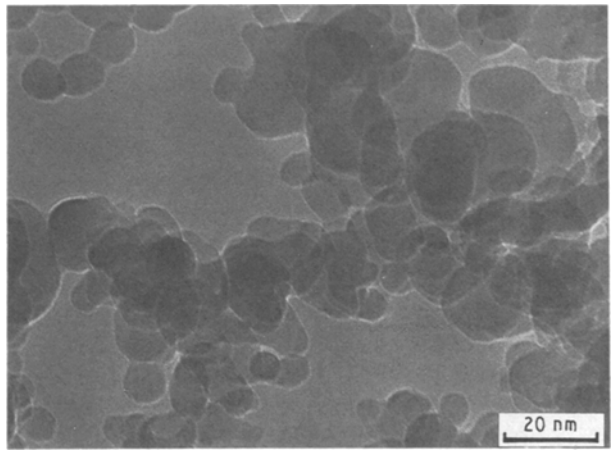

Figure 1 Ultrafine powder prepared by a thermal Plasma CVD. There is no contrast from an amorphous phase. The average particle size is about 30 nm.

2. Experimental procedure

2.1. Powder characterization

A hybrid plasma was used to prepare ultrafine Si_3N_4 powder as reported previously [11]. Its quenching rate was very fast, from 10^5 to 10^6 K s^{-1}. Such a rapid quenching is very useful in preparing ultrafine Si_3N_4 powder, because very small nucleations are considered difficult to grow to larger particles. The ultrafine Si_3N_4 powder observed by TEM showed no contrast due to an amorphous phase, as shown in Fig. 1, because the electron diffraction pattern was a halo. However, powder observed at high magnification showed something approaching a different contrast in the particles. The average size of the powder was 0.03 μm. It was heated at 500 °C for 1 h in flowing nitrogen, in order to remove unreactive materials such as NH_3 and HCl. It was again heat treated at 1300–1450 °C for 1–4 h in an nitrogen stream, producing a crystallized powder. A transmission electron micrograph of the resultant powder is shown in Fig. 2. Some particles have a black contrast and others only a faint one: the former particles diffracted the incident electron beams, whereas the others did not. The diffracted beams are usually eliminated with an objective aperture under the specimen particles and, as a resultant, only the transmitted beams contribute to form a bright-field image. At high magnification, we can

0022–2461

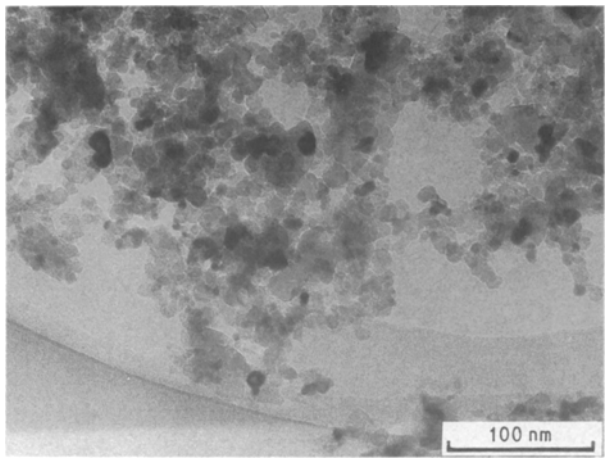

Figure 2 Particles with dark contrast in crystallized Si_3N_4 powder. The dark particles diffract the incident electron beams.

clearly see an image with lattice fringes in a particle, as shown in Fig. 3. The lattice fringes of lie in different directions, as indicated by the arrows, therefore the particle would be composed of a few grains. Such a particle may be formed by sintering of agglomerated particles during quenching. The surface layer of about 2 nm is amorphous, which has not been observed in S_3N_4 powders prepared by conventional methods. Thus the powder obtained in this work may show a relatively high concentration of structural features.

2.2. Sintering

The crystallized powder was slightly yellow with an average size of about 200 nm. After heat treatment, Si_3N_4 powder in various degrees of crystallization was obtained corresponding to the temperature and time of the heat treatment. The crystallization of the Si_3N_4 obtained was determined by a method previously developed by Yamada *et al.* [12].

The crystallized Si_3N_4 powder was mixed with 5 wt % Al_2O_3 and 5 wt % Y_2O_3 in an ethanol solution in an Si_3N_4 mortar for 30 min. After drying the powder, it was pressed at 250 kg cm^{-2} and then hydrostatically pressed at 2 ton cm^{-2}. The sintering temperature was from 1550–1800 °C in a nitrogen stream. A high-frequency-induced furnace was used for sintering [11]. The specimens were placed in a carbon crucible with a powder bed of 50 wt % Si_3N_4 + 40 wt % h-BN + 10 wt % additives. The h-BN was a lubricant, which assisted removal of the sintered body from the carbon crucible. The specimen was then heated to a given temperature at a constant heating rate about 20 °C min^{-1}. However, if amorphous powder was heated at this rate, many cracks were generated in the sintered body because of very high shrinkage. Therefore, the amorphous powder was heated at a slower rate of 10 °C min^{-1}. The colour of the sintered bodies was grey. The relative density was measured by the Archimedes' method. The green density of a compact was calculated from its size and weight. One side of the sintered body was polished to a mirror surface on a copper disc using diamond powder. The other side of the body was then polished again to about 100 μm, and finally carefully polished to about 30 μm. The resultant film then ion-thinned for observation with a TEM operating at 200 kV.

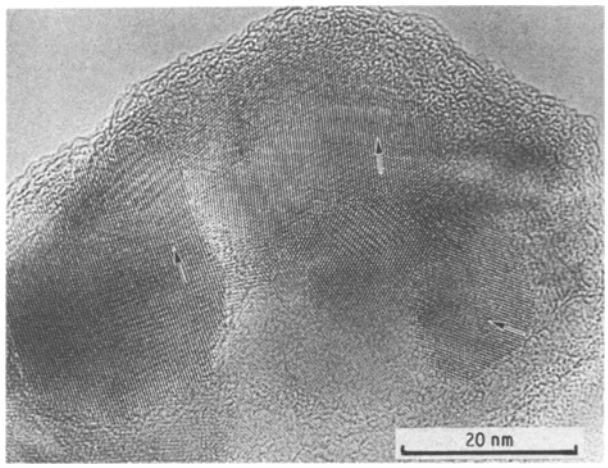

Figure 3 A high-resolution micrograph of a crystallized powder showing several grains, as indicated by arrows. The surface of the particle is amorphous.

3. Results and discussion

It is well known that the value of the green density is very important for subsequent sinterability, therefore, first we checked the relationship between the green density and the degree of crystallization, as shown in Fig. 4. The green density increases over the range from 0%–40% crystallization. The Si_3N_4 powder in various degrees of crystallization was sintered at 1650 °C for 1 h. The relative density of the sintered bodies obtained was plotted against the various crystallization states, as shown in Fig. 5. From the figure it is apparent that the density was strongly dependent on the crystallization, particularly from 0%–10%. It was nearly constant for a crystallization higher than 10%. Therefore, the 70% crystallization powder was used for sintering. The different tendencies of the curves in Figs 4 and 5 may be related to the homogeneous mixing of Si_3N_4 with additives, as discussed later.

It is interesting to compare the sinterability of Si_3N_4 obtained by plasma processing with that prepared by other processes, such as by the decomposition of

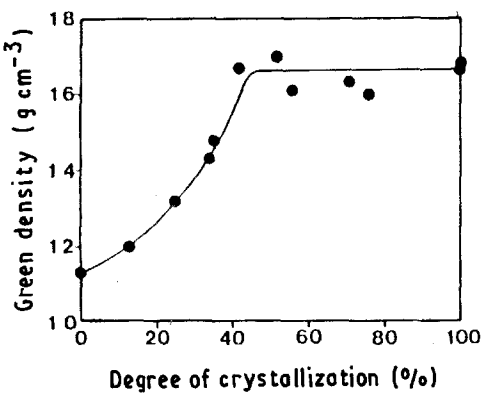

Figure 4 The relationship between relative density and crystallization.

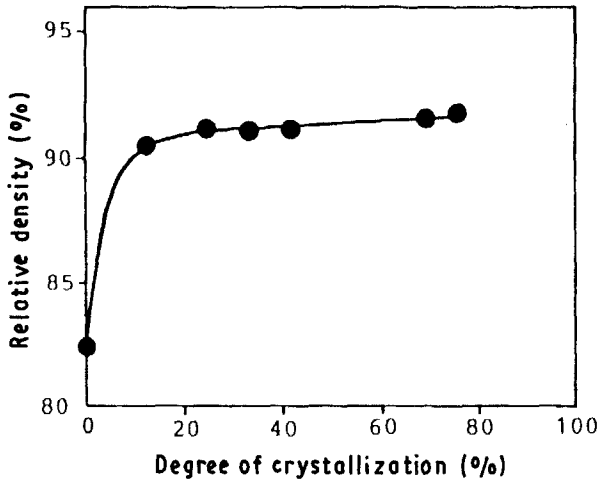

Figure 5 Relationship between relative density and crystallization in a body sintered at 1650 °C for 1 h in nitrogen.

silicon imido, vapour deposition, nitridation of silicon. These physical properties were listed in previous paper [11].

The Si_3N_4 powder was mixed with 5 wt % Al_2O_3 and 5 wt % Y_2O_3 in an Si_3N_4 mortar with ethanol solution for 30 min. It was hydrostatically pressed at 2 ton cm^{-2} (199 MPa) and sintered at 1550–1800 °C for 1 h in flowing nitrogen with the high-frequency-induced furnace mentioned before. The specimen obtained from the plasma method was used for comparison with the specimens obtained from other methods.

The sintering data obtained are shown in Fig. 6, where D, D′, I, R, C and P are commercially available Si_3N_4 powder prepared by direct nitridation of silicon, decomposition of silicon imido, nitridation of SiO_2, vapour deposition and that obtained here by thermal plasma, respectively. As can be seen in the figure, each sample has a maximum density at 1700 °C. The increase of relative density from 1550–1700 °C indicates the effect of ion diffusion through the liquid phase on densification. On the other hand, the decrease in relative density above 1700 °C may show the effect the decomposition and evaporation on dedensification.

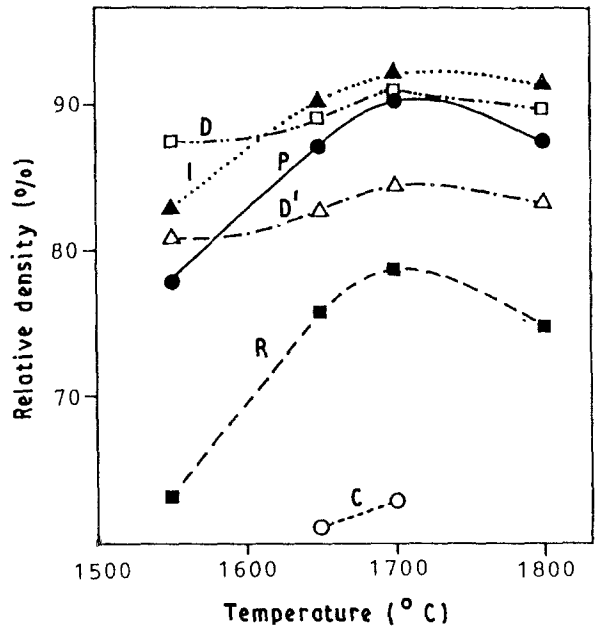

Figure 6 Relationship between relative density and temperature for various specimens; D. D′, I, R, C and P are direct nitridation of silicon, decomposition of silicon imido, nitridation of SiO_2, vapour deposition, and thermal plasma CVD (this work), respectively.

In comparison with other specimens, D and D′ show a different dependency of shrinkage curves on temperature, i.e. the relative density is almost constant, regardless of temperature. This is related to the high concentration of impurities, such as iron and particularly calcium. For this, a liquid phase would be formed at temperatures lower than 1550 °C. The liquid phase should contribute to the densification at such a low temperature.

The difference between D and D′ is related to be the large size of D′ particles. Specimen C has the lowest density of all. It is difficult to compact to high green density because of the needle shape of the particles. The relatively low density of R would be related to its large particle size. According to Fig. 6, Specimens D and I are very sinterable, and they sinter to high density at 1700 °C. Specimen P has a slightly lower density than those of Specimens D and I. The difference between them is not very large, therefore this may be related to the inhomogeneous mixing of the specimens with the sintering additives. In fact, there is no difference between their sintered densities, when they are homogeneously mixed with sintering additives in the following way.

Specimens D, I, and P with 5 wt % Al_2O_3 and 5 wt % Y_2O_3 were ball-milled in a plastic crucible for 12 h using Si_3N_4 balls in an alcohol solution. They were then dried, and isostatically pressed at 2 ton cm^{-2} (199 MPa); then the resultant specimens were sintered at 1700 °C for 1 h in a stream of nitrogen. As a result, all the specimens have approximately the same density. Therefore, the discrepancy in the sintering densification between Specimens D, I and P, as shown in Fig. 6, is concluded to be due to the inhomogeneous mixing with the sintering additives. Thus, homogeneous mixing is very important for correct densification, because sintering is a topochemical reaction.

Fig. 7 shows a scanning electron micrograph of a sintered body in Specimen P. Clearly from the figure,

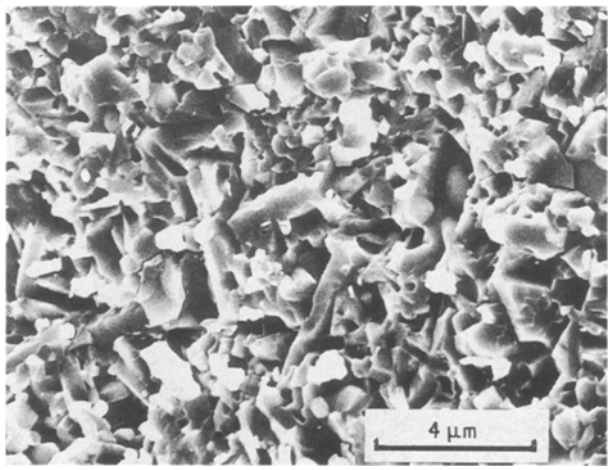

Figure 7 Scanning electron micrograph of the fracture surface of sintered Si_3N_4 prepared in this work.

its density looks high. The aspect ratio of average grains is about 4. However, it is difficult to discuss the detailed microstructure, such as wetness between a grain and liquid phase, a grain boundary, and so on. Fig. 8 shows transmission electron micrographs of Specimen P observed at low magnification. As can be seen in the figure, all grains are wetted with a liquid phase with dark contrast. The grains have sharp crystal habits, for instance, which observed from the $\langle 0001 \rangle$ zone axis indicates clearly hexagonal planes, as shown in Fig. 9. This suggests that grain growth in sintering took place by diffusional transfer through a liquid. The grain corner is curved, due to the tension of Si_3N_4. The liquid phase was always in dark contrast, because the heavy metal of yttrium is considered to scatter incident electron beams. The slightly white contrast in the liquid phase around the grain may indicate glasses, due to phase separation by electron radiation.

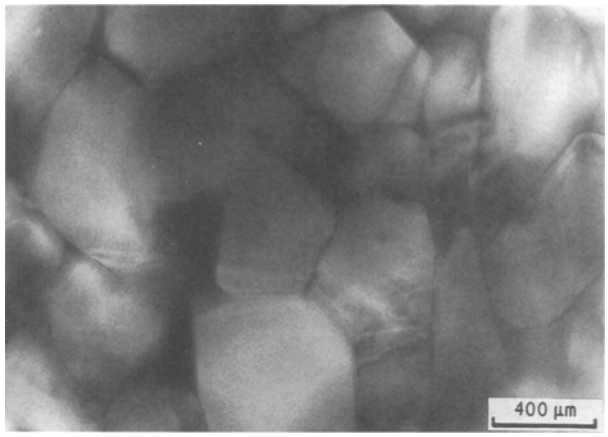

Figure 8 Transmission electron micrograph of a sintered body indicating that all the grains are wet with a liquid phase.

Fig. 10 shows a grain boundary in Si_3N_4 observed in high resolution. The surface of the lower grain has a (0001) plane, which is perpendicular to the incident electron beams. The upper grain is inclined a few degree against the lower grain. In the figure, we can see lattice fringes of 0.65 nm; however, no kind of lattice defect could be observed. Although the width of a grain boundary is considered to be a few micrometres

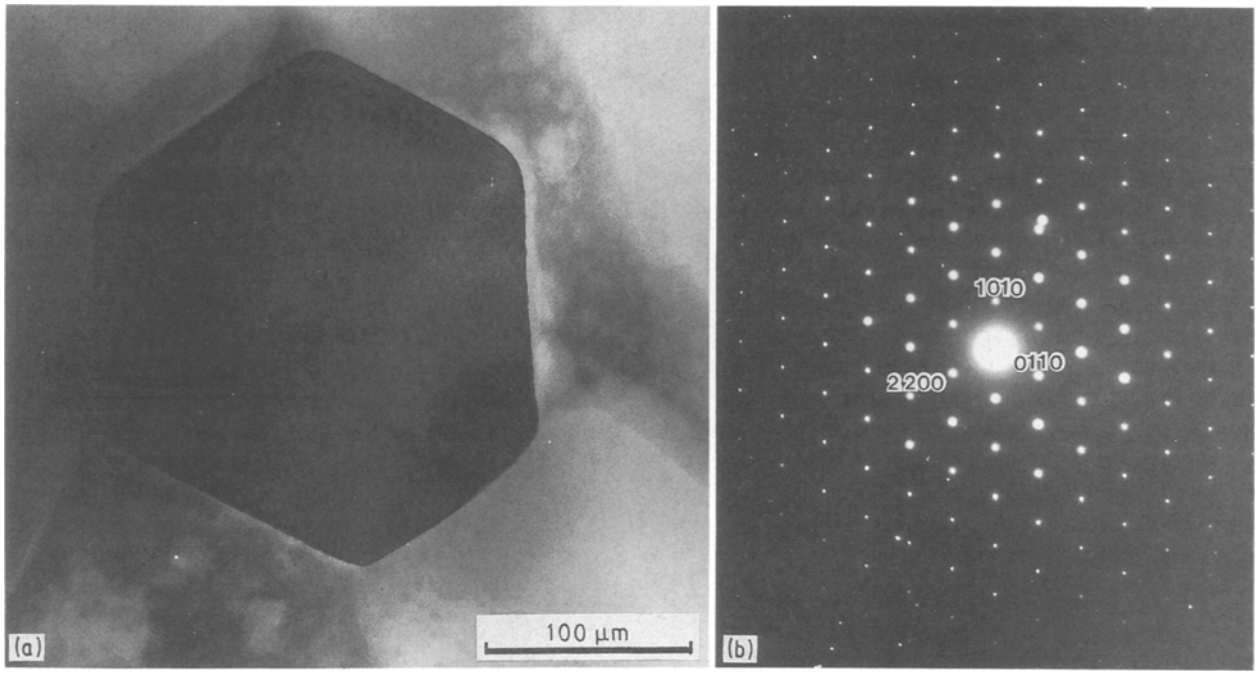

Figure 9 (a) Grain observed from the $\langle 0001 \rangle$ direction as indicated in the diffraction pattern (b).

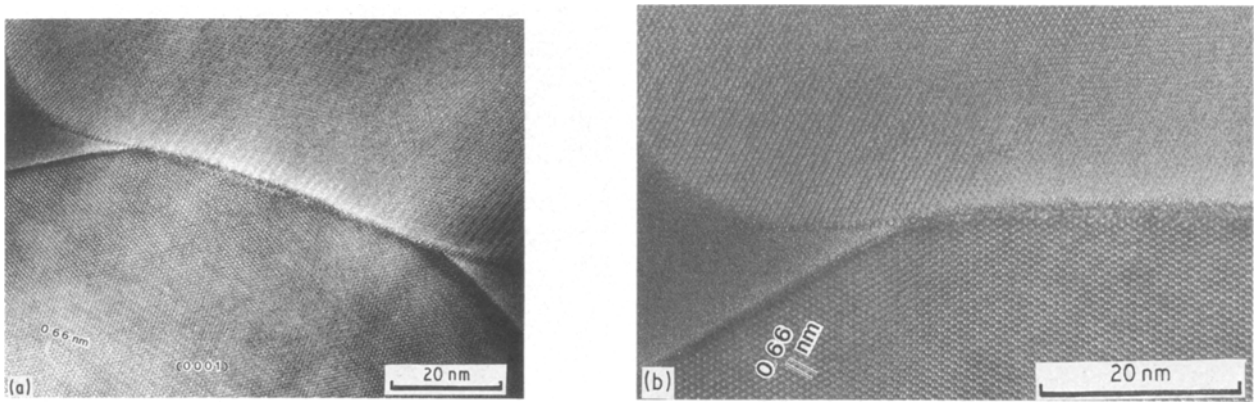

Figure 10 High-resolution transmission electron micrographs of a grain boundary between two grains. Both micrographs (a) and (b) clearly indicate that the dihedral angle is smaller than 30°. This may suggest that the grain boundary is wet with liquid phase.

in alumina and magnesia, the width from our data is very narrow, about 20 nm. The dihedral angle is from 20°–30°. This indicates that the grain-boundary energy is higher than the liquid–solid interfacial energy, which would suggest that the grain boundary is wet with liquid phase. In fact, it can be seen that the dark contrast of the liquid phase penetrates into the grain boundary as shown in Fig. 11, when the boundary was observed under other diffraction conditions. A high concentration of the liquid-phase components could also be detected at the boundary using an analytical transmission microscope.

Some grain boundaries have direct bonding between two grains. This kind of boundary may be considered to be a specific one, a so-called coincident boundary, as shown in Fig. 12. In this case, the grain-boundary energy is smaller than the liquid–solid interfacial energy. For this, the dihedral angle must be larger than 120°. In fact, the dihedral angle observed here was about 90°, the grain boundary would not be parallel to incident electron beams.

It is said that sintered bodies of Si_3N_4 with Al_2O_3 and Y_2O_3 usually have a high fracture toughness, compared with those containing other sintering additives. So far, the reasons for this have been discussed through empirical information. However, we consider from EDX analysis that Y-apatite ($Y_{10}(SiO_4)_6N_2$) should be present in the liquid phase, where the aluminium ions would partially substitute the Y sites. If we observe the liquid phase with a TEM in high resolution, lattice fringes can be seen in the direction indicated by an arrow, as shown in Fig. 13. EDX analysis indicates that aluminium ions made a solid solution with the Si_3N_4 but, on the other hand, only a small amount of yttrium ions make a solid solution with it, as shown in Fig. 14. The apatite would be generated during the cooling stage from the sintering temperature; thus the cooling rate is very important.

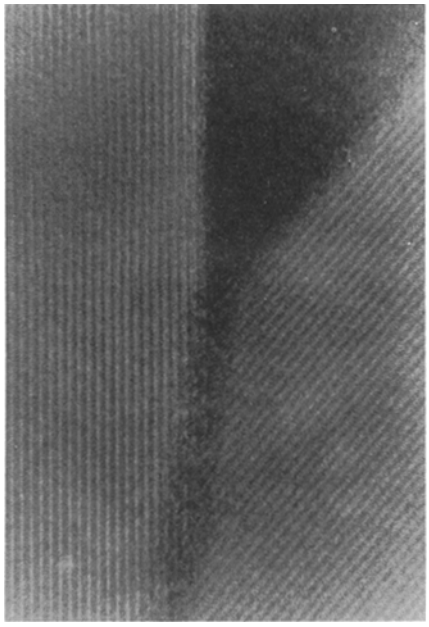

Figure 11 High-resolution transmission electron micrograph observed under different conditions, indicating that liquid phase penetrates into the grain boundary.

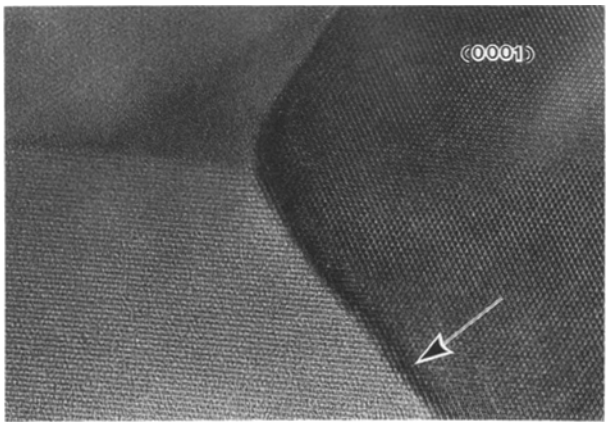

Figure 12 High-resolution transmission electron micrograph of a coincident boundary (arrowed) showing that the dihedral angle is large, about 90°, the boundary energy would be smaller than the liquid–solid interfacial energy.

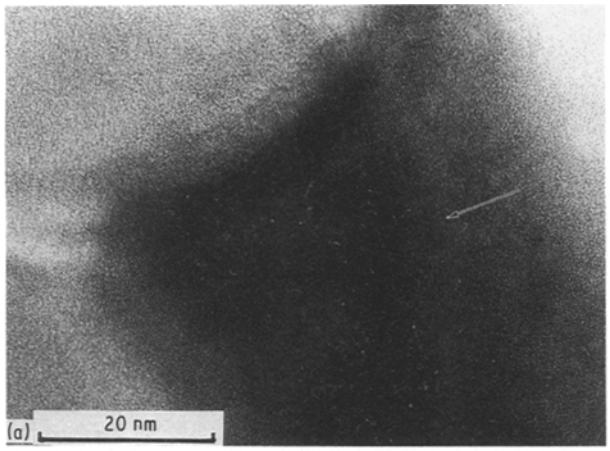

Figure 13 High-resolution transmission electron micrographs of a liquid phase showing (a) the lattice fringes in the liquid phase. (b) Higher magnification.

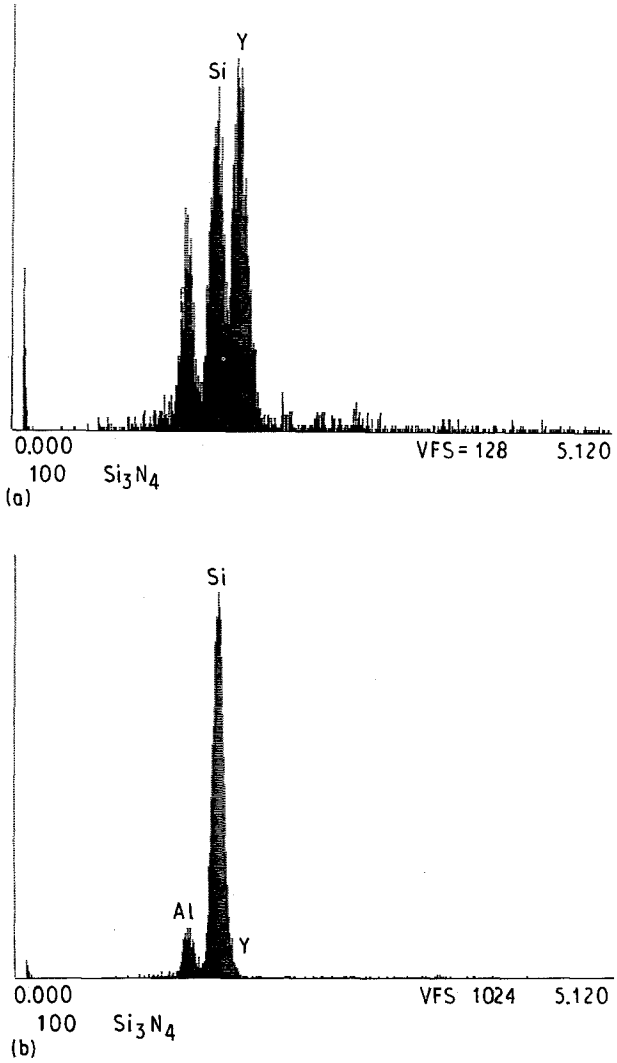

Figure 14 EDX data showing a high concentration of both (a) aluminium and yttrium in the liquid phase, and (b) a low concentration of aluminium in Si_3N_4. This would suggest that aluminium ions make a solid solution with Si_3N_4.

In this connection, Falk and Dunlop [13] reported from a study of the crystallization of the liquid phase in an Si_3N_4 material by post-sintering heat treatments, that the glassy phase in Si_3N_4 fabricated by nitridation during sintering, using Y_2O_3 and Al_2O_2 as sintering additives, can be substantially crystallized by post-heat-treatments in air at 1100–1400 °C. They found Y-apatite phase in a specimen heat-treated at 1200 °C and the amorphous phase at 1400 °C.

In summary, ultrafine Si_3N_4 with an average grain size of 30 nm was prepared by the thermal plasma CVD method. The green and sintered densities were greatly related to the crystallization of the powder. The sinterability was almost constant in a sample with a crystallization higher than 40%. It was difficult to obtain a high green density as easily as with conventional samples. However, if the ultrafine Si_3N_4 was homogeneously mixed with sintering additives, it sintered to 98% density in a nitrogen atmosphere. Scanning electron micrographs showed that the sintered bodies were dense and the aspect ratio of the grains was about 4. The microstructures observed by TEM indicated that the grains with crystal habits were wet with liquid phase. This suggests that the sintering and grain growth of Si_3N_4 took place by diffusional transfer of ions through the liquid phase. High-resolution transmission electron micrographs showed two kinds of grain boundaries: one was wet with liquid phase and the other was a direct bonding one, a so-called coincident grain boundary. During cooling from the sintering temperature, a liquid phase was considered to change into a crystal phase of apatite.

References

1. G. R. TERWILLIGER and F. F. LANGE, *J. Amer. Ceram. Soc.* **57** (1974) 25.
2. *Idem., J. Mater Sci.* **10** (1975) 1169.
3. R. E. LOEHMAN and D. J. ROWCLIFFE, *J. Amer. Ceram. Soc.* **63** (1980) 144.
4. M. MITOMO, *J. Mater. Sci.* **11** (1976) 1103.
5. H. F. PRIEST, G. L. PRIEST and G. E. GAZA, *J. Amer. Ceram. Soc.* **60** (1977) 81.
6. K. H. JACK, in "Nitrogen Ceramics", edited by F. L. Riley (Nordhoff-Leyden, 1977) p. 109.
7. W. H. RHODES, *J. Amer. Ceram. Soc.* **64** (1981) 19.
8. C. GRESKOVICH and J. H. ROSOLOWSKI, *ibid.* **59** (1976) 336.
9. S. FUTAKI, K. SHIRAISHI and T. YOSHIDA, *Yogyo-Kyokai-Shi* **90** (1985) 7.
10. L. K. L. FALK, R. POMPE and G. L. DUNLOP, *J. Mater. Sci.* **20** (1985) 3545.
11. M. FUTAKI, Y. SHIMIZU, K. SHIRAISHI, Y. MORIYOSHI, T. SATO and T. SAKAI, *ibid.* **22** (1987) 4331.
12. T. YAMADA, K. MASUNAGA, T. KUNISAWA and Y. KOTOKU, *Yogyo-Kyokai-Shi* **93** (1985) 394.
13. L. K. L. FALK and G. L. DUNLOP, *J. Mater. Sci.* **22** (1987) 4369.

Received 18 April
and accepted 5 August 1991